Automated dynamic characteristics estimation of highway bridge under ambient vibration by block companion form realization

Bashir Ahmad JAWAID *, Takatoshi OKABAYASHI**, Md. Rajab ALI *** and Toshihiro OKUMATSU ****

* M. of Eng., Graduate student, Nagasaki University, Bunkyou machi 1-14, Nagasaki 852-8521
** Dr. of Eng., Professor, Dept. of Civil Eng., Nagasaki University, Bunkyou machi 1-14, Nagasaki 852-8521
*** Graduate student, Nagasaki University, Bunkyou machi 1-14, Nagasaki 852-8521
****M. of Eng., Research associate, Dept. of Civil Eng., Nagasaki University, Bunkyou machi 1-14, Nagasaki 852-8521

In this research, vibration characteristics are estimated from the ambient vibration of highway bridge by the block companion form realization theory. Two methods are stated herein such as formulation of block companion system matrix; (i) directly from block Hankel matrix, (ii) from ARMA model parameter **G** through Yule-Walker equation. These methods have applied to a 152m long Langer bridge and its dynamic characteristics were estimated automatically from multipoint measurement of ambient vibration. As the ambient vibration characteristics affect the estimation accuracy, two different cases were taken into consideration and the estimation accuracy was evaluated.

Key Words: Ambient vibration, dynamic characteristics estimation, ARMA model, realization theory

1. Introduction

System identification by modal analysis[1)] has brought the opportunity to accurately estimate structural dynamic characteristics (frequency, damping constant, and vibration mode). In order to obtain bridge dynamic characteristics[2) 3)] by modal analysis method, ambient vibration is assumed as white noise or external force with a spectrum structure of certain characteristics. In this method, structural dynamic characteristics is obtained from experimental data through theoretical transfer function by curve fitting using non-linear least square method. On the other hand, dynamic characteristics could be estimated using AR or ARMA model[4) ~ 6)] from time series analysis without consideration of a physical model.

In the recent years, computation of system matrix[7) ~ 11)] by realization theories become easy because calculation of large matrix at high speed can be done with the help of high performance personal computer. Authors proposed automated estimation of bridge dynamic characteristics from ambient vibration using block companion form realization method[12)].

Discretized state equation is transferred to block companion state equation by observability matrix and ARMA model is formulated by corresponding block companion form. However, the block companion form state equation introduces a standard realization theory that is formulated from the relation of block Hankel matrix which is similar to Ibrahim time-domain method[13) 14)]. In stochastic realization theory, block Hankel matrix is formed by covariance matrix, though in deterministic realization theory, block Hankel matrix is formed by Markov parameter. In addition, the relation between the block Hankel matrix formulated by covariance matrix and the system matrix by the block companion form has been included with the Yule-Walker equation, from which classic multi-dimensional ARMA model coefficient is obtained. In the future, as an inverse problem of structural identification from measurement data, ARMA model will be an important method [15)] for the modeling of existing structures.

This research achieves dynamic characteristics estimation with ambient vibration of a highway bridge by the stochastic block companion form realization theory. Two methods are stated herein for formulation of block companion system matrix; (i) directly from block Hankel matrix, (ii) from ARMA model parameter **G** through Yule-Walker equation.

The methods have applied to an existing bridge for automated estimation of dynamic characteristics. The 152 m long Kabashima bridge, situated in Nagasaki city, was selected as object bridge and its dynamic characteristics were estimated from the multipoint measurement of ambient vibration. As the ambient vibration characteristics affect the estimation accuracy, two different cases, such as stationary ambient vibration with wind force and non-stationary ambient vibration intermitting moving vehicles were taken into consideration for dynamic characteristics estimation.

2. State space representation of equation of motion

2.1 State space representation of equation of motion

Bridge structures can be modeled by FEM and their dynamic characteristics are expressed through n DOF system of following equation of motion for external forces acting on r nodes out of n nodes.

$$\mathbf{m}\ddot{\mathbf{z}}(t)+\mathbf{c}\dot{\mathbf{z}}(t)+\mathbf{k}\mathbf{z}(t)=\mathbf{d}\mathbf{f}(t) \tag{1}$$

where $\mathbf{z}(t)\in\mathbf{R}^n$ and $\mathbf{f}(t)\in\mathbf{R}^r$ are displacement and external force vector. $\mathbf{m}\in\mathbf{R}^{nxn}$, $\mathbf{c}\in\mathbf{R}^{nxn}$ and $\mathbf{k}\in\mathbf{R}^{nxn}$ are mass, damping and stiffness matrices for the structural system, respectively. Moreover, $\mathbf{d}\in\mathbf{R}^{n\times r}$ is the vector of input force when acting on r nodes. General viscous damping is considered in this study. For gradual change of $\mathbf{f}(\tau)$ within $t_k\le\tau\le t_{k+1}=t_k+T$, in this time interval $\mathbf{f}(\tau)$ is constant vector as $\mathbf{f}(k)$:

$$\mathbf{f}(\tau)=\mathbf{f}(k) \qquad (t_k\le\tau\le t_{k+1}) \tag{2}$$

similarly, proceeding with discretization of displacement $\mathbf{z}(t)$ and velocity $\dot{\mathbf{z}}(t)$ into $\mathbf{z}(k)$ and $\dot{\mathbf{z}}(k)$. External force $\mathbf{p}(k)\in\mathbf{R}^{2n}$ and state variable $\mathbf{x}(k)\in\mathbf{R}^{2n}$ can be represented as

$$\mathbf{x}(k)=\begin{bmatrix}\mathbf{z}(k)\\ \dot{\mathbf{z}}(k)\end{bmatrix} \qquad \mathbf{p}(t)=\begin{bmatrix}\mathbf{d}\\ \mathbf{0}\end{bmatrix}\mathbf{f}(k) \tag{3}$$

$\mathbf{y}(k)\in\mathbf{R}^m$ is expressed as m point observation of structure in terms of displacement $\mathbf{z}(k)$ and velocity $\dot{\mathbf{z}}(k)$ and discretized state equation is formulated from Eq. (1) as

$$\mathbf{x}(k+1)=\mathbf{A}\mathbf{x}(k)+\mathbf{B}\mathbf{f}(k) \tag{4-1}$$
$$\mathbf{y}(k)=\mathbf{C}\mathbf{x}(k) \tag{4-2}$$

and system matrix, external force matrix of linear state equation are

$$\overline{\mathbf{A}}=\begin{bmatrix}\mathbf{m} & \mathbf{c}\\ \mathbf{0} & \mathbf{m}\end{bmatrix}^{-1}\begin{bmatrix}-\mathbf{k} & \mathbf{0}\\ \mathbf{0} & \mathbf{m}\end{bmatrix},\quad \overline{\mathbf{B}}=\begin{bmatrix}\mathbf{m} & \mathbf{c}\\ \mathbf{c} & \mathbf{m}\end{bmatrix}^{-1}\begin{bmatrix}\mathbf{d}\\ \mathbf{0}\end{bmatrix} \tag{5}$$

where, $\overline{\mathbf{A}}\in\mathbf{R}^{2n\times 2n}$, $\overline{\mathbf{B}}\in\mathbf{R}^{2n\times r}$.

Coefficient matrices for discretized state equation are

$$\mathbf{A}=e^{\overline{\mathbf{A}}(t_{k+1}-t_k)}=e^{\overline{\mathbf{A}}T}$$

$$\mathbf{B}=\int_{t_{;k}}^{t_{k+1}}e^{\overline{\mathbf{A}}(t_{k+1}-\tau)}d\tau \quad \mathbf{B}=(e^{\overline{\mathbf{A}}T}-\mathbf{I})\overline{\mathbf{A}\mathbf{B}} \tag{6}$$

where $\mathbf{A}\in\mathbf{R}^{2n\times 2n}$, $\mathbf{B}\in\mathbf{R}^{2n\times r}$ and observation matrix $\mathbf{C}\in\mathbf{R}^{m\times 2n}$ can be found from observation value $\mathbf{y}(t)$ and extracted from the state variable $\mathbf{x}(t)$.

2.2 Block companion form state equation

Observability matrix of discretized state Eq. (4) is

$$\mathbf{P}_p=\begin{bmatrix}\mathbf{C}\\ \mathbf{CA}\\ \\ \mathbf{CA}^{p-1}\end{bmatrix} \tag{7}$$

the system is observable for $rank(\mathbf{P}_p)=2n$ and $m\times p=2n$. Next relationship can be formulated from the characteristics of multi-dimensional observability (Appendix A):

$$\mathbf{CA}^p=-\mathbf{G}_p\mathbf{C}-\mathbf{G}_{p-1}\mathbf{CA}\cdots\ \ \cdots-\mathbf{G}_1\mathbf{CA}^{p-1} \tag{8}$$

where $\mathbf{G}_s\in\mathbf{R}^{m\times m}$ is coefficient matrix. The system matrix $\mathbf{A}$ is thus converted to generalized observable system matrix as follows:

$$\mathbf{P}_p\mathbf{A}=\begin{bmatrix}\mathbf{CA}\\ \mathbf{CA}^2\\ \vdots\\ \mathbf{CA}^p\end{bmatrix}=\begin{bmatrix}\mathbf{0} & \mathbf{I} & \mathbf{0} & \cdots & \mathbf{0}\\ \mathbf{0} & \mathbf{0} & \mathbf{I} & \cdots & \mathbf{0}\\ \vdots & \vdots & \vdots & \ddots & \vdots\\ -\mathbf{G}_p & -\mathbf{G}_{p-1} & -\mathbf{G}_{p-2} & \cdots & -\mathbf{G}_1\end{bmatrix}\begin{bmatrix}\mathbf{C}\\ \mathbf{CA}\\ \vdots\\ \mathbf{CA}^{p-1}\end{bmatrix}=\hat{\mathbf{A}}\mathbf{P}_p \tag{9}$$

then, discretized state variable in terms of observation matrix $\mathbf{P}_p$ can be:

$$\mathbf{P}_p\mathbf{x}(k)=\hat{\mathbf{x}}(k) \tag{10}$$

Therefore, block companion form state equation will be:

$$\hat{\mathbf{x}}(k+1)=\hat{\mathbf{A}}\hat{\mathbf{x}}(k)+\hat{\mathbf{B}}\mathbf{f}(k) \tag{11-1}$$
$$\mathbf{y}(k)=\hat{\mathbf{C}}\hat{\mathbf{x}}(k) \tag{11-2}$$

where, force matrix and observation matrix are respectively

$$\hat{\mathbf{B}}=\mathbf{P}_p\mathbf{B}=\begin{bmatrix}\mathbf{CB}\\ \mathbf{CAB}\\ \vdots\\ \mathbf{CA}^{p-1}\mathbf{B}\end{bmatrix}=\begin{bmatrix}\hat{\mathbf{B}}_1\\ \vdots\\ \hat{\mathbf{B}}_{p-1}\\ \hat{\mathbf{B}}_p\end{bmatrix} \tag{12}$$

and

$$\hat{\mathbf{C}}=\mathbf{CP}_p{}^{-1}=\begin{bmatrix}\mathbf{I} & \mathbf{0} & \cdots & \mathbf{0}\end{bmatrix}. \tag{13}$$

2.3 Ambient vibration modeling and auto correlation function of observation process

Ambient vibration is modeled by random vibration theory for linear dynamic system including unknown external force acting on structure. External force is assumed as stationary white noise process $\mathbf{w}(k)\in\mathbf{R}^r$ with zero mean value. The covariance of $\mathbf{w}(k)$ can be expressed:

$$E\left[\mathbf{w}(k+l)\mathbf{w}^T(l)\right]=\begin{cases}\Sigma_{\mathbf{w}} & (l=0)\\ \mathbf{0} & (l\ne 0)\end{cases} \tag{14}$$

where $E[\ ]$ is mathematical mean value and $\Sigma_{\mathbf{w}}\in\mathbf{R}^{r\times r}$. The mean value of external force and initial boundary condition are to be zero. In this case the solution process $\mathbf{x}(k)$ is stationary process with zero mean value and the covariance is as

$$\mathbf{R}_{\mathbf{x}}(k) = E\left[\mathbf{x}(k)\mathbf{x}(k)^T\right] \tag{15}$$

Covariance equation of solution process is formulated by substituting Eq. (4-1) into Eq. (15) and using the relation of Eq. (14). For $k \to \infty$, $\mathbf{R}_{\mathbf{x}}(k)$ is $\mathbf{R}_{\mathbf{x}}$ and covariance of the solution process is obtained as

$$\mathbf{R}_{\mathbf{x}} = \mathbf{A}\mathbf{R}_{\mathbf{x}}\mathbf{A}^T + \mathbf{B}\mathbf{Q}\mathbf{B}^T \tag{16}$$

where $\mathbf{Q}$ is as follows:

$$\mathbf{Q} = E\left[\mathbf{w}(k)\mathbf{w}(k)^T\right] \tag{17}$$

The auto correlation of solution process for stationary process is the time invariant of $\mathbf{x}(l+k)$ and $\mathbf{x}(l)$:

$$\mathbf{R}_{\mathbf{xx}}(k) = E\left[\mathbf{x}(l+k)\mathbf{x}(l)^T\right] \tag{18}$$

Next relation is formulated by substituting Eq. (4-1) into Eq. (18) and using the Eq. (14), we can obtain:

$$\mathbf{R}_{\mathbf{xx}}(k) = \mathbf{A}^k\mathbf{R}_{\mathbf{x}} \qquad (l \geq 0) \tag{19}$$

The covariance matrix $\mathbf{R}_{\mathbf{yy}}(k)$ of observation data is expressed as follows according to the Eq. (4-2) and Eq. (19) :

$$\mathbf{R}_{\mathbf{yy}}(k) = \begin{cases} \mathbf{C}\mathbf{R}_x\mathbf{C}^T & l = 0 \\ \mathbf{C}\mathbf{A}^{k-1}\hat{\mathbf{B}} & k > 1 \end{cases} \tag{20}$$

where $\hat{\mathbf{B}} = \mathbf{A}\mathbf{R}_{\mathbf{x}}\mathbf{C}^T$.

3. Relation between Hankel matrix and block companion system matrix

3.1 Decomposition of Hankel matrix

Defining $(p+1)\times(q+1)$ block Hankel matrix:

$$\mathbf{H}_{p+1,q+1}(k) = \mathbf{P}_{p+1}\mathbf{A}^k\mathbf{Q}_{q+1} \tag{21}$$

where, $\mathbf{P}_{p+1} = \begin{bmatrix} \mathbf{C} \\ \mathbf{CA} \\ \vdots \\ \mathbf{CA}^p \end{bmatrix}$, $\quad \mathbf{Q}_{q+1} = \begin{bmatrix} \mathbf{B} & \mathbf{AB} & \cdots & \mathbf{A}^q\mathbf{B} \end{bmatrix}$ (22)

The matrix $\mathbf{P}_{p+1}$ is called extended observability matrix and the matrix $\mathbf{Q}_{q+1}$ is called extended controllability matrix. The minimum dimension of the state matrix is $n \times n$ for n order system. In that case the rank of Hankel matrix is n .

3.2 Estimation of block companion system matrix $\hat{\mathbf{A}}$

The next equation is formulated from extended observability matrix stated in Eq. (8)

$$\mathbf{P}_p\mathbf{A}^{s+1} = \begin{bmatrix} \mathbf{CA}^{s+1} \\ \mathbf{CA}^{s+2} \\ \vdots \\ \mathbf{CA}^{s+p} \end{bmatrix} = \begin{bmatrix} \mathbf{0} & \mathbf{I} & \mathbf{0} & \cdots & \mathbf{0} \\ \mathbf{0} & \mathbf{0} & \mathbf{I} & \cdots & \mathbf{0} \\ \vdots & \vdots & \vdots & \ddots & \vdots \\ -\mathbf{G}_p & -\mathbf{G}_{p-1} & -\mathbf{G}_{p-2} & \cdots & -\mathbf{G}_1 \end{bmatrix} \begin{bmatrix} \mathbf{CA}^{s} \\ \mathbf{CA}^{s+1} \\ \vdots \\ \mathbf{CA}^{s+p-1} \end{bmatrix} = \hat{\mathbf{A}}\mathbf{P}_p\mathbf{A}^s \tag{23}$$

right multiplying $\mathbf{Q}_q$ on both terms of Eq.(23) yields

$$\mathbf{P}_p\mathbf{A}^{s+1}\mathbf{Q}_q = \hat{\mathbf{A}}\mathbf{P}_p\mathbf{A}^s\mathbf{Q}_q \tag{24}$$

Using the relationship of Hankel matrix written in Eq. (21):

$$\mathbf{H}(s) = \hat{\mathbf{A}}\mathbf{H}(s-1) \tag{25}$$

for simplification, $\mathbf{H}_{p,q}(s)$ is expressed as $\mathbf{H}(s)$ and detail form of Eq. (25) will be:

$$\begin{bmatrix} \boldsymbol{\Lambda}(s+1) & \cdots & \cdots & \boldsymbol{\Lambda}(s+q) \\ \vdots & & & \\ \vdots & & & \\ \boldsymbol{\Lambda}(s+p) & \cdots & \cdots & \boldsymbol{\Lambda}(s+p+q) \end{bmatrix} = \hat{\mathbf{A}} \begin{bmatrix} \boldsymbol{\Lambda}(s) & \cdots & \cdots & \boldsymbol{\Lambda}(s+q-1) \\ \vdots & & & \\ \vdots & & & \\ \boldsymbol{\Lambda}(s+p-1) & \cdots & \cdots & \boldsymbol{\Lambda}(s+p+q-2) \end{bmatrix} \tag{26}$$

(1) For obtaining block companion system matrix $\hat{\mathbf{A}}$

Block companion matrix $\hat{\mathbf{A}}$ can be formulated from Eq. (26) using least square method as below:

$$\hat{\mathbf{A}} = \mathbf{H}(s)\mathbf{H}(s-1)^T(\mathbf{H}(s-1)\mathbf{H}(s-1)^T)^{-1} \tag{27}$$

(2) Obtaining $\mathbf{G} = \lfloor -\mathbf{G}_1 \quad -\mathbf{G}_2 \quad \cdots \quad -\mathbf{G}_p \rfloor$ as elements of $\hat{\mathbf{A}}$

If $\mathbf{T}_1 = \mathbf{H}(s-1)$ and $\mathbf{T}_2^{\in mx(m(q-1)row)}$ are the lowest blocks of $\mathbf{H}(s)$, then Eq. (26) would be similar as the Yule-Walker Eq. (B-6) of Appendix B and $\mathbf{G}$ can be found as

$$\mathbf{G} = \mathbf{T}_2(\mathbf{T}_1\mathbf{T}_1^T)^{-1} \tag{28}$$

$\hat{\mathbf{A}}$ can be formed by $\mathbf{G}$ according to Eq. (9). In addition in the both cases, $\hat{\mathbf{A}}$ and $\mathbf{G}$ can be obtained using singular value decomposition.

4. Dynamic characteristics estimation

4.1 Covariance matrix estimation using measured signal

To obtain Eq. (26), it is necessary to calculate the covariance matrix of the measured signal. Measured signal is assumed to have ergodicity characteristics and covariance matrix of observation process was calculated according to the time average. In case of m dimensional discrete measured signal, covariance of observed signal $\hat{\mathbf{y}}(k)$ is

$$\hat{\boldsymbol{\Lambda}}(r) = \frac{1}{N-r}\sum_{k=1}^{N-r}\hat{\mathbf{y}}(k+r)\hat{\mathbf{y}}^T(k) \qquad (r = s \cdots s+q) \tag{29}$$

$$\hat{\boldsymbol{\Lambda}}(-r) = \hat{\boldsymbol{\Lambda}}^T(r) \tag{30}$$

4.2 Modal analysis of block companion matrix

(1) Frequency and damping constant estimation

For similar relation of $\hat{\mathbf{A}}$ and $\mathbf{A}$, eigenvalue and eigenvector $\boldsymbol{\Psi}$ of $\hat{\mathbf{A}}$ can be obtained by eigenvalue analysis:

$$\boldsymbol{\Psi}^T\hat{\mathbf{A}}\boldsymbol{\Psi} = e^{\Lambda\Delta} = \boldsymbol{\Gamma} = \begin{bmatrix} \boldsymbol{\mu} & \mathbf{0} \\ \mathbf{0} & \boldsymbol{\mu}^* \end{bmatrix} \tag{31}$$

where $\mu^*_k = e^{\lambda^*_k\Delta}$ and $\mu_k = e^{\lambda_k\Delta}$ are complex conjugate. λ_k and λ_k^* are the k^{th} order eigenvalues of motion equation stated in Eq. (1) and will be as

$$\lambda_k = -\sigma_k + i\omega_{dk} \quad , \quad \lambda_k^* = -\sigma_k - i\omega_{dk} \tag{32}$$

For proportional damping system, real and imaginary part represents modal damping and natural frequency as

$$\sigma_k = h_k \omega_k \, , \quad \omega_{dk} = \omega_k \sqrt{1-h^2} \tag{33}$$

The frequency and modal damping of the structural system are obtained from the eigenvalue of $\hat{\mathbf{A}}$:

$$\omega_{dk} = \frac{1}{\Delta} \tan^{-1} \left| \frac{\mu_k - \bar{\mu}_k}{\mu_k + \bar{\mu}_k} \right| \quad , \quad \sigma_k = -\frac{1}{2\Delta} \ln(\mu_k \bar{\mu}_k) \tag{34}$$

for proportional damping system, k^{th} order natural frequency ω_k and modal damping h_k can be expressed by Eq. (35):

$$\omega_k = \sqrt{\omega_{dk}{}^2 + \sigma_k{}^2} \, , \quad h_k = \sigma_k / \omega_k \tag{35}$$

(2) Vibration mode estimation system

Eigen equation of matrix **A** for discretized state equation is as follows:

$$(\mathbf{A} - \mathbf{\Gamma})\mathbf{\Psi} = \mathbf{0} \tag{36}$$

left multiplying of the observation matrix $\mathbf{P}_p$ into Eq. (36) will convert the related eigen equation of system matrix $\hat{\mathbf{A}}$:

$$(\mathbf{P}_p \mathbf{A} \mathbf{P}_p{}^{-1} - \mathbf{P}_p \mathbf{\Lambda} \mathbf{P}_p{}^{-1}) \mathbf{P}_p \mathbf{\Psi} = \mathbf{0}$$

$$(\hat{\mathbf{A}} - \mathbf{\Gamma})\mathbf{P}_p \mathbf{\Psi} = (\hat{\mathbf{A}} - \mathbf{\Lambda})\mathbf{\Phi} = \mathbf{0} \tag{37}$$

therefore, the eigenvector of $\hat{\mathbf{A}}$ will be:

$$\mathbf{\Phi} = \begin{bmatrix} \mathbf{C} \\ \mathbf{CA} \\ \vdots \\ \mathbf{CA}^{s-1} \end{bmatrix} \mathbf{\Psi} = \begin{bmatrix} \mathbf{C\Psi} \\ \mathbf{C\Psi\Psi}^{-1}\mathbf{A\Psi} \\ \vdots \\ \mathbf{C\Psi}(\mathbf{\Psi}^{-1}\mathbf{A\Psi})^{s-1} \end{bmatrix} = \begin{bmatrix} \hat{\mathbf{\Psi}} \\ \hat{\mathbf{\Psi}}\mathbf{\Lambda} \\ \vdots \\ \hat{\mathbf{\Psi}}\mathbf{\Lambda}^{s-1} \end{bmatrix} \tag{38}$$

upper m rows of $\mathbf{\Phi}$ are the eigenvectors of system matrix $\hat{\mathbf{A}}$ for mode vectors corresponding m points observation matrix of state space Eq. (4).

(3) Extraction of frequency, modal damping, and mode shapes

a) Estimation of frequency and damping constant

The eigenvalues of discrete system of Eq. (32) can be rewritten as

$$\lambda_k = e^{-h_k \omega_k \Delta} (\cos \omega_d T + i \sin \omega_d T) \tag{39}$$

these eigenvalues are displayed on the complex plane by

$$r = e^{-h_k \omega_k T}$$

$$\theta = \tan^{-1} \omega_{dk} T \cong \tan^{-1} \omega_k T \tag{40}$$

for small value of damping constant $\omega_{dk} \cong \omega_k$. Therefore, frequency $\omega_{\max}$ and modal damping $h_{\max}$ are desirable to be calculated. The extraction range of the frequency and modal damping will be as following:

$$e^{-h_{\max} \omega_{\max} T} < r < 1 \qquad 0 < \theta < \tan^{-1} \omega_{\max} T \tag{41}$$

b) Vibration mode estimation

The vibration modes can be derived from the eigenvector of system matrix $\hat{\mathbf{A}}$ using Eq. (38) for m point observation:

$$\hat{\mathbf{\Psi}} = \begin{bmatrix} \psi_{11} & \cdots & \psi_{1m} \\ \vdots & \ddots & \vdots \\ \psi_{m1} & \cdots & \psi_{mm} \end{bmatrix} \tag{42}$$

Eigenvalue λ_k is calculated by realization method, then corresponding eigen mode can be obtained from that eigenvalue as

$$\hat{\mathbf{\Psi}}_k = \begin{bmatrix} \psi_{1k} \\ \\ \psi_{mk} \end{bmatrix} \tag{43}$$

5. Automatic measurement with ambient vibration

5.1 Object bridge

A Langer bridge, situated in Nagasaki city, was selected as object bridge and its dynamic characteristics were estimated from the multipoint measurement of ambient vibration. Figure 1 shows the front view and Table 1 shows the properties of Kabashima Bridge.

Fig.1 Kabashima bridge

Table 1 Properties of Kabashima bridge

Bridge Type	Steel Langar Truss Bridge
Length (Center Span)	227 m (152 m)
Width	7.5 m
Construction Year	1986

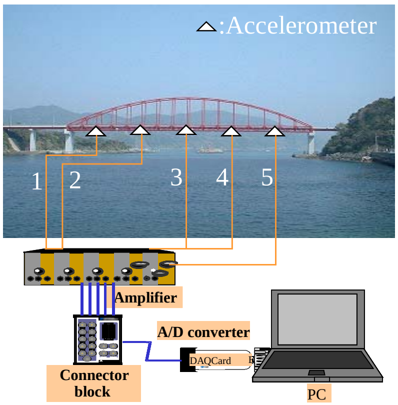

(a) Vertical acceleration measurement sensors installation

(b) Torsional measurement sensors installation
Fig. 2 Measurement apparatus installation to the bridge

Table 2 Measurement apparatus

	Type (Manufacturer)	Specicfication
A/D converter	DAQ Card-6062E (National Instruments)	Analogue input: 16ch , 12bit
Accelerometer	710 (TEAC)	Sensitivity: 300 (mv/m/s^2) Frequency response: 0.02-200Hz
Amplifier	SA-611 (TEAC)	
Personal computer	CF-19 (Panasonic)	OS:Windows XP Pro

5.2 Experiment

The bridge's ambient vibration measurement was conducted with accelerometer. Five accelerometers were installed on the bridge to obtain vertical acceleration simultaneously as shown in Figure 2(a). Two accelerometers were installed at the middle of bridge span for recording the torsional vibration data as shown in Figure 2 (b). Table 2 shows the measurement apparatus used during the experiment. Measurement program was developed with LabVIEW 7.5 (National Instruments).

We conducted offline analysis to estimate the bridge's dynamic characteristics. 1200 consecutive time history data per channel are hired to obtain one dynamic characteristic for 30 second according to data sampling frequency, which was selected as 100Hz. By 50 time repetitions of the operation, we could evaluate the bridge's dynamic characteristics change visually.

The indicator to evaluate dynamic characteristics is controlled by characteristics of ambient vibration. The bridge is surrounded by strong wind condition because it locates at the very top of the Nagasaki Peninsula. This means the ambient vibration observed on the bridge is influenced by wind conditions.

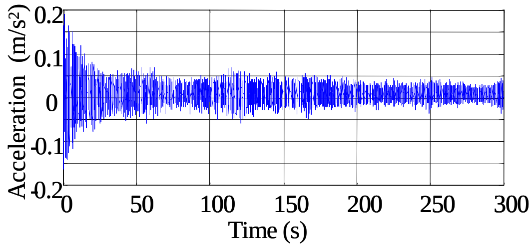

(a) Acceleration data (Case 1)

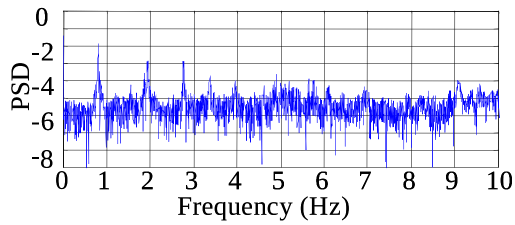

(b) Power spectrum density (Case 1)
Fig. 3 Ambient vibration data (Case 1)

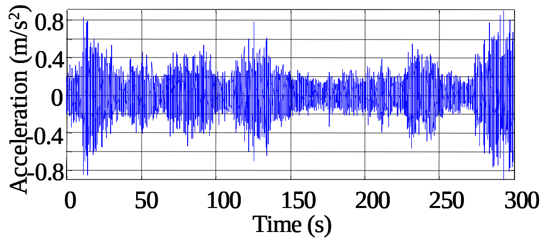

(a) Acceleration data (Case2)

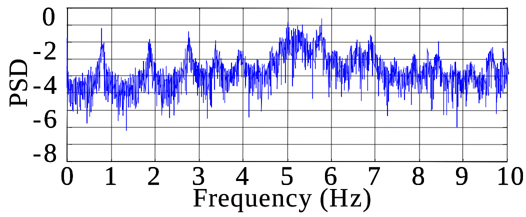

(b) Power spectrum density (Case 2)
Fig. 4 Ambient vibration data (Case2)

Naturally, by moving vehicles on the bridge, the bridge vibration will be induced strongly. Ambient vibration by wind load constantly induces low frequency vibration to the bridge, where ambient vibration by moving vehicles induces relatively high power 3 to 5 Hz frequency, which means the automobile's vibration characteristics. Accordingly, two cases were focused in this paper. One is the ambient vibration data induced by constant wind load, and the other is the ambient vibration induced by moving vehicles. The former case was indicated in Figure 3 (a) and (b) with its power spectrum density as recorded vertical acceleration under the strong wind conditions in June, 2007. The latter case was indicated in Figure 4 (a) and (b) with its power spectral density as recorded under the moving vehicles.

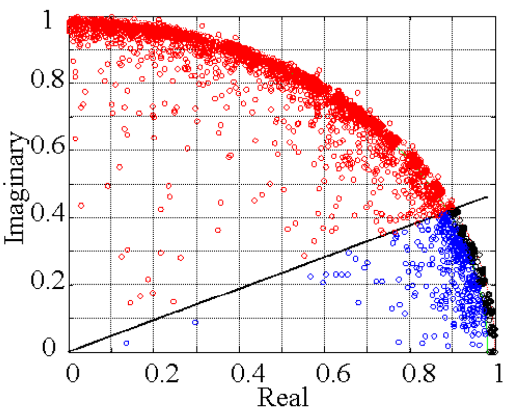

Fig. 5 Extraction of eigenvalue

The both data were recorded with the No.1 sensor location that is shown in Figure 2 (a). The consecutive series of data were used for estimating dynamic characteristics. By comparing each power spectrum density of the Figure 3(b) and Figure 4(b), it is recognized that 3 to 7 Hz frequencies have induced under vehicles intermitting.

6. Automatic measurement for stationary vibration (Case 1)

6.1 Extraction of eigenvalue

Eigenvalues from system matrix $\hat{\mathbf{A}}$ were plotted in a complex plane as shown in Figure 5. The maximum frequency and modal damping restricted the extraction range for eigenvalue. The complex eigenvalues extracted from this region have considered for frequency and modal damping estimation. In addition, vibration modes are estimated from the eigenvector corresponding to the eigenvalues.

6.2 Comparison of the estimation method

In this study, two methods were taken into consideration. The first method was stated in Eq. (26). In this case, dynamic characteristics were estimated from the eigenvalue of companion matrix in Eq. (27), which was directly formulated from Hankel matrix. Second method was stated in Eq. (28). The results from ambient vibration data were almost same for both methods. Therefore, in this study, first method was employed for dynamic characteristics estimation due to the simplicity of calculation.

6.3 Estimation results (Case 1)

(1) Estimation of frequency

The dynamic characteristics were estimated based on the ambient vibration data, which was measured on a comparatively windy day. The data sampling frequency of acquiring ambient vibration was set as 100 Hz. 1200 consective

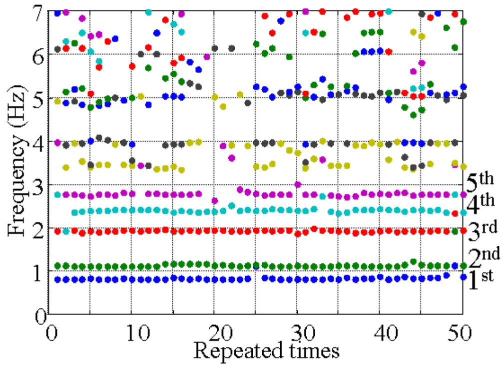

Fig. 6 Estimation of frequency

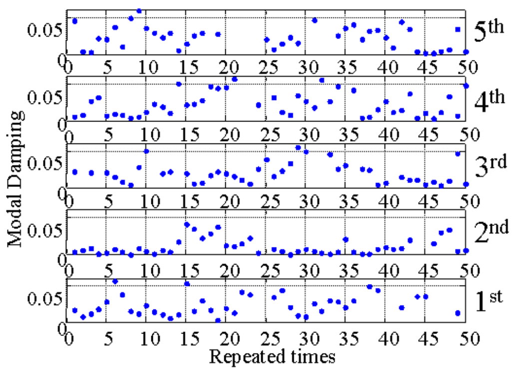

Fig.7 Estimation of modal damping

Table 3 Estimation accuracy of dynamic characteristics

Mode order	Frequency (Hz)			Modal damping		
	Mean value	Standard deviation	Coefficient of variation (%)	Mean value	Standard deviation	Coefficient of variation (%)
1st	0.840	0.060	7.143	0.043	0.044	102.326
2nd	1.143	0.115	10.061	0.014	0.023	164.286
3rd	1.946	0.061	3.135	0.031	0.023	74.194
4th	2.416	0.113	4.677	0.029	0.026	89.655
5th	2.948	0.527	17.877	0.034	0.026	76.471

data were processed for each time estimation and the process was continued for 50 times repeatedly as shown in Figure 6. The figure shows that frequency up to 5th mode can be estimated stably. According to the ambient vibration measurement, shown in Figure 3, continuous estimation is possible for stationary ambient vibration. Moreover estimated frequencies between 4Hz to 5Hz also gathered in order, but we can see that those estimation accuracies are comparatively lower than up to 5th mode.

(2) Estimation of modal damping

Figure 7 shows the estimated values of modal damping. Based on the experimental result it can be seen that the modal damping estimation can be realized for well-excited vibration modes. However deviation of estimated modal damping is larger than the deviation in frequency estimation. So this result would be compared with other method. Figure 7 indicates that the modal damping is within 0.05, and as a general evaluation criterion, it is possible to estimate modal damping.

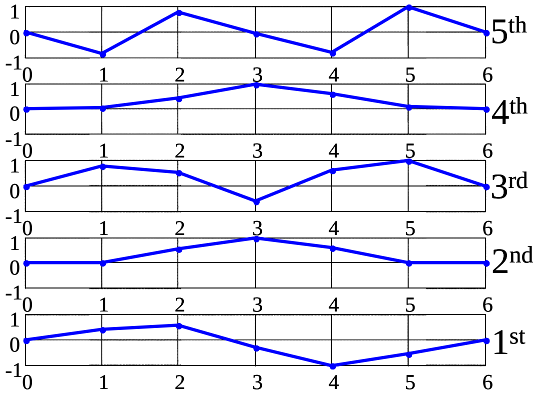

Fig. 8 Estimation of vibration mode shapes

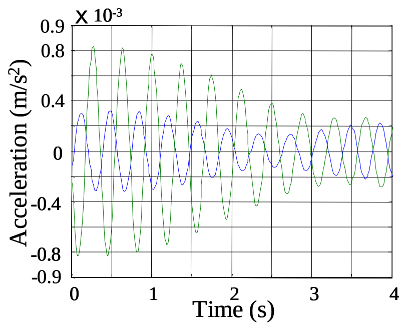

Fig. 9 Torsional vibration measurement

Consideration is added for the mean value and the coefficient of variation of the modal damping corresponding to frequency.

(3) Estimation accuracy of dynamic characteristics

Table 3 shows mean value, standard deviation and coefficient of variation regarding the estimated frequency and modal damping for 50 repeated times. Up to now, the statistical analysis for clearly estimated frequency and modal damping is not targeted, as the measurement for each time and their processing is time consuming. To forecast the deterioration of the bridge caused by structural damage or global aging from the change in the vibration characteristics, it is necessary to know their change statistically for control of maintenance. For this reason automated dynamic characteristics estimation and processing of large number of observations data are thought to be an important.

Coefficients of variation of frequencies up to 4^{th} mode were within 10%. This indicates that high accuracy estimation of frequencies has realized. The mean value of 3^{rd} mode frequency is 1.946Hz and coefficient of variation is 3.13% i.e. estimated value is within the limit of 1.946 ± 0.061 Hz. Coefficient of variation of frequency for 5^{th} mode is within 20%, which means estimation accuracy is a little bit lower.

Estimated values for modal damping were between 0.014 ~0.043 and their coefficient of variation is among 74~164%. It can be thought that comparatively steady estimation has realized with the accuracy of about 100% for the coefficient of variation.

(4) Estimation of vibration mode

Figure 8 shows the estimated vibration mode shapes. According to the realization theories, we can obtain the higher order mode shapes. But actually, it is thought that more than the five vibration mode shapes could not be estimated clearly because those are dependent on the number and location of sensors. The obtained vibration mode shapes are the average of 50 times estimation and the maximum value of each mode shape set as one. The five estimated mode shapes were similar in shape of the typical Langer truss bridge except 4^{th} mode shape. The 2^{nd} mode shape shows typical arch effect and it becomes symmetric mode shape. 2^{nd} and 4^{th} mode shapes are same in shape. This is because of the omission of torsional mode by placing the accelerometer along the bridge length at the time of experiment, and consequently it was not able to detect torsional mode. Figure 9 shows the vibration phase for the torsional measurement. This was measured by placing accelerometer along the width bound of bridge at the middle of bridge span as shown in Figure 2(b). Therefore it can be said that 4^{th} one is torsional mode shape.

Thus, a multi-dimensional AR model and block companion form realization are able to observe the vibration mode shapes easily by the multipoint simultaneous observation compare to the modal analysis method.

7. Automatic measurement for non-stationary ambient vibration (Case 2)

Next, we deal with traffic load, which was induced bridge vibration case (Case 2). Acceleration data recorded under the traffic flow is shown in Figure 4(a). The figure shows some peaks related moving vehicles. As shown in Figure 4(b), according to the automobile's natural frequency of 3 to 5Hz, the bridge vibration is induced with not only near the automobile's natural frequency modes, but also the higher modes (5 to 7Hz). From this standpoint, under the consecutive measurement, estimation results may scatter according to intermittent vehicles.

7.1 Estimation of frequency

50 times frequency estimation results were shown in Figure 10. Comparing the result with Figure 6, which is wind load induced ambient vibration, we can see that there are some lacks or changes in frequency estimation in lower frequency modes from 1^{st} to 5^{th}. On the other hand, we can see that relatively higher modes, such as around 4, 5, 6, and 7Hz, have induced. By repeating these measurements and by using stable estimation results, reliable natural frequency estimation will be realized. Thus, intermitting vehicles would affect on estimation results' changes in frequency especially in higher modes. It should be observed stable ambient vibration to obtain steady estimation results.

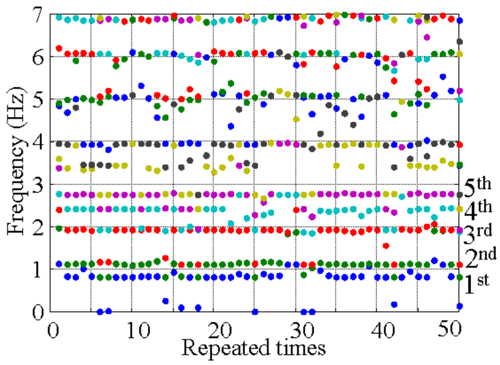

Fig.10 Estimation of frequency

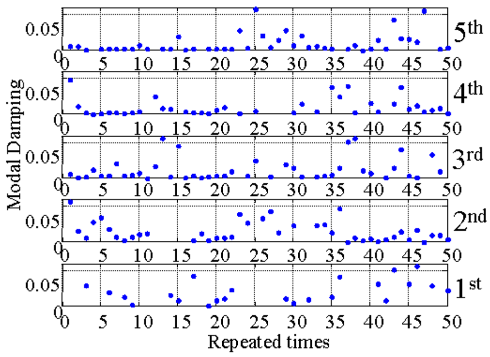

Fig.11 Estimation of modal damping

Table. 4 Estimation accuracy of dynamic characteristics

Mode order	Frequency (Hz)			Modal damping		
	Mean value	Standard deviation	Coefficient of variation (%)	Mean value	Standard deviation	Coefficient of variation (%)
1st	0.726	0.340	46.832	0.191	0.296	154.974
2nd	1.145	0.280	24.454	0.022	0.033	150.000
3rd	1.785	0.346	19.384	0.016	0.028	175.000
4th	2.305	0.267	11.584	0.026	0.036	138.462
5th	2.765	0.435	15.732	0.015	0.027	180.000

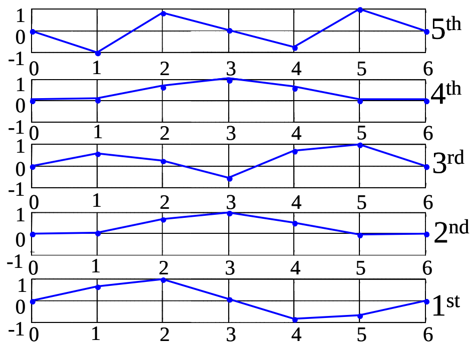

Fig. 12 Estimation of vibration mode shapes

7.2 Estimation of modal damping

Estimation process of modal damping is shown in Figure 11. From the estimation results, we can see the 1st mode's modal damping is relatively or extremely big, whereas the rest are estimated small. This means that dynamic characteristics have not been estimated stably, the modal damping, which is very sensitive for estimating the dynamic characteristics, remains unstable. To evaluate this phenomenon, statistical operation for estimation results of frequency and modal damping were performed.

7.3 Estimation accuracy of dynamic characteristics

Statistical operation results for estimating frequency and modal damping are shown in Table 4. As for the frequency estimation, the result of coefficient of variation changes from 11 to 46 %. It is relatively higher number compared with Case1, especially in 1st mode of 46.8%. This means that there exist errors for estimating lower frequency mode in this bridge under the inconstant vehicles intermitting. As for 4th and 5th mode, each coefficient of variation is relatively small and realized good estimation.

As for the estimation of modal damping, the result of 1st mode shows 0.191 of mean value and 155% of coefficient of variation. The mean value overrate the actual phenomenon and also the coefficient of variation remained high. As shown above, same with the case for frequency estimation, the system could not estimate lower frequency mode. We found that the coefficient of variation shows big value in Case 2 compared to Case 1 for estimated modal damping.

Thus, it is important to evaluate the characteristics of ambient vibration beforehand to realize automatic bridge vibration characteristics estimation.

7.4 Estimation of vibration mode

Figure 12 shows estimated vibration mode shapes, which is mean value of consecutive 50 time repetition. As shown in this figure, same as Case 1, good estimations were realized. The reason why the 2nd and 4th mode shapes are same, same with Figure 8, the 4th mode shape represents torsional vibration mode shape.

8. Conclusions

In this paper, automatic estimation method of dynamic characteristics proposed by the stochastic block companion form realization with ambient vibration. The summary of the paper is as follows.

(1) Formulation of block companion system matrix from block Hankel matrix, and Yule-Walker equation were indicated and dynamic characteristics estimation-equations were derived for simultaneous multipoint ambient vibration measurement of the bridge.

(2) This method was applied to the ambient vibration measurement for the existing bridge and the same estimation results were found for stochastic block companion form realization method and ARMA model through Yule- Walker equation. In addition, stochastic block companion form realization method can be used for dynamic characteristics estimation due to its simplicity of programming.

(3) Stochastic block companion form realization method was applied to obtain the dynamic characteristics of existing bridge for multipoint ambient vibration measurement. Dynamic characteristics were estimated for the stationary state of ambient vibration. Especially, automated estimation of vibration mode is the efficiency of this method.
(4) Dynamic characteristics were estimated for stationary state of ambient vibration caused by wind force and non-stationary ambient vibration by moving vehicles. Stable and continuous estimation of dynamic characteristics was possible for stationary ambient vibration.
(5) In case of non-stationary ambient vibration, some lacks or changes of frequency have caused in lower modes. Also, we recognized that structure's frequency will be affected with not only near vehicle's frequencies but also higher frequency mode of the structure. These results indicate that we should evaluate environmental effects beforehand for estimating structural dynamic characteristics precisely.

Appendix A : Derivation of equations

$$\mathbf{CA}^{p} = -\mathbf{G}_{p}\mathbf{C} - \cdots\cdots - \mathbf{G}_{2}\mathbf{CA}^{p-2} - \mathbf{G}_{1}\mathbf{CA}^{p-1}$$

Singular value decomposition of Hankel matrix will be as:

$$\mathbf{H}_{p+1,q+1}(\mathbf{0}) = \mathbf{USV}^{T} = \begin{bmatrix}\mathbf{U}_{n} & \mathbf{U}_{0}\end{bmatrix}\begin{bmatrix}\mathbf{S}_{n} & \mathbf{0}\\ \mathbf{0} & \mathbf{0}\end{bmatrix}\begin{bmatrix}\mathbf{V}_{n}^{T}\\ \mathbf{V}_{0}^{T}\end{bmatrix} = \mathbf{U}_{n}\mathbf{S}_{n}\mathbf{V}_{n} \quad \text{(A-1)}$$

where the columns of $\mathbf{U}$ and $\mathbf{V}$ are orthogonal, and $\mathbf{S}$ is a rectangular matrix. Right and left multiplication of $\mathbf{U}^{T}$ and $\mathbf{V}^{T}$ on Eq. (A-1) yields:

$$\begin{aligned}\mathbf{U}^{T}\mathbf{H}_{p+1,q+1}(\mathbf{0})\mathbf{V}^{T} &= \begin{bmatrix}\mathbf{U}_{n}^{T}\\ \mathbf{U}_{0}^{T}\end{bmatrix}\mathbf{P}_{p+1}\mathbf{Q}_{q+1}\begin{bmatrix}\mathbf{V}_{n} & \mathbf{V}_{0}\end{bmatrix}\\ &= \begin{bmatrix}\mathbf{U}_{n}^{T}\mathbf{P}_{p+1}\mathbf{Q}_{q+1}\mathbf{V}_{n} & \mathbf{U}_{n}^{T}\mathbf{P}_{p+1}\mathbf{Q}_{q+1}\mathbf{V}_{0}\\ \mathbf{U}_{0}^{T}\mathbf{P}_{p+}\mathbf{Q}_{q+1}\mathbf{V}_{n} & \mathbf{U}_{0}^{T}\mathbf{P}_{p+1}\mathbf{Q}_{q+1}\mathbf{V}_{0}\end{bmatrix} = \begin{bmatrix}\mathbf{S}_{n} & \mathbf{0}\\ \mathbf{0} & \mathbf{0}\end{bmatrix}\end{aligned} \quad \text{(A-2)}$$

The next relations are obtained from Eq. (A-2):

$$\mathbf{U}_{n}^{T}\mathbf{P}_{p+1}\mathbf{Q}_{q+1}\mathbf{V}_{0} = 0 \quad \mathbf{U}_{0}^{T}\mathbf{P}_{p+1}\mathbf{Q}_{q+1}\mathbf{V}_{n} = 0 \quad \text{(A-3)}$$

The following relation can be written as

$$\mathbf{U}_{0}^{T}\mathbf{P}_{p+1} = 0 \quad \text{(A-4)}$$

$$\mathbf{U}_{0}^{T} = \begin{bmatrix}\mathbf{U}_{01}^{T} & \cdots & \cdots & \mathbf{U}_{0p+1}^{T}\end{bmatrix} \quad \text{(A-5)}$$

where $\mathbf{U}_{0s}^{T}\ (s = 1\cdots p+1) \in \mathbf{R}^{(mp+m-n)\times m}$.
The next relation is obtained by expanding Eq.(A-4):

$$\mathbf{U}_{01}^{T}\mathbf{C} + \cdots \cdots + \mathbf{U}_{0p}^{T}\mathbf{CA}^{p-1} + \mathbf{U}_{0p+1}^{T}\mathbf{CA}^{p} = 0 \quad \text{(A-6)}$$

left multiplying general inverse matrix $(\mathbf{U}_{0p+1}^{T})^{+}$ of $\mathbf{U}_{0p+1}^{T}$ on Eq. (A-6) and introducing coefficient

$$\mathbf{G}_{l} = (\mathbf{U}_{0p+1}^{T})^{+}\mathbf{U}_{0p-l+1}^{T} \quad (l = 1\cdots p)$$

and the following relation is introduced

$$\mathbf{CA}^{p} = -\mathbf{G}_{p}\mathbf{C} - \cdots\cdots - \mathbf{G}_{2}\mathbf{CA}^{p-2} - \mathbf{G}_{1}\mathbf{CA}^{p-1}. \quad \text{(A-7)}$$

Appendix B: Relation between block companion form realization and AR model

(1) Transformation of state equation to multidimensional ARMA model

The multidimensional ARMA model can be obtained by block companion matrix from Eq.(11). ARMA model regarding block companion matrix expressed in Eq.(9) is to be

$$\begin{aligned}&\mathbf{y}(k+p) - \mathbf{G}_{1}\mathbf{y}(k+(p-1)) - \mathbf{G}_{2}\mathbf{y}(k+(p-2)) - \cdots - \mathbf{G}_{p}\mathbf{y}(k)\\ &= \mathbf{R}_{1}\mathbf{f}(k+p-1) + \mathbf{R}_{2}\mathbf{f}(k+p-2) + \cdots\cdots + \mathbf{R}_{p}\mathbf{f}(k)\end{aligned} \quad \text{(B-1)}$$

where, $\mathbf{R}_{1} \sim \mathbf{R}_{s}$ are external force coefficients.
As an approximation of multidimensional ARMA model in Eq. (B-1), model order is considered as greater than p

$$\mathbf{y}(k) + \sum_{l=1}^{p}\mathbf{G}_{l}\mathbf{y}(k-l) = \mathbf{e}(k) \quad \text{(B-2)}$$

and the auto correlation of white noise $\mathbf{e}(l)$ with $\mathbf{0}$ mean value formulated as

$$E\left[\mathbf{e}(k+l)\mathbf{e}^{T}(l)\right] = \begin{cases}\mathbf{\Sigma}_{\mathbf{e}} & (l = 0)\\ \mathbf{0} & (l \neq 0)\end{cases} \quad \text{(B-3)}$$

where, $\mathbf{\Sigma}_{\mathbf{e}} \in \mathbf{R}^{m\times m}$.

(2) Estimation of multidimensional AR model parameter by Yule-Walker equation

Assuming $\mathbf{y}(k)$ as m multipoint measurement sampling signal. For a stationary time series, the covariance matrix of the time series is given from the definition by the next expression:

$$E\left[\mathbf{y}(k+s)\mathbf{y}^{T}(k)\right] = E\left[\mathbf{y}(k)\mathbf{y}^{T}(k-s)\right] = \mathbf{\Lambda}(s) \quad \text{(B-4)}$$

where, $E[\ ]$ is mathematical mean.
Right multiplying $\mathbf{y}(k-r)^{T}$ into Eq.(B-4) and taking mathematical mean, we can get covariance equation of observation signal:

$$\mathbf{\Lambda}(r) + \mathbf{G}_{1}\mathbf{\Lambda}(r-1) + \cdots + \mathbf{G}_{p}\mathbf{\Lambda}(r-p) = \mathbf{0} \quad \text{(B-5)}$$

thus Yule –walker equation is obtained for $r = 1 \sim q$.
To increase the size of equations from unknown numbers, Eq.(B-5) is composed for $q > m\times p$ and $r = s+p \sim s+p+q-1$ where s is starting point:

$$\begin{aligned}&\begin{bmatrix}-\mathbf{G}_{p} & -\mathbf{G}_{p-1} \cdots & -\mathbf{G}_{1}\end{bmatrix}\begin{bmatrix}\mathbf{\Lambda}(s) & \mathbf{\Lambda}(s+1) & \cdots & \mathbf{\Lambda}(s+p) & \cdots & \mathbf{\Lambda}(s+q-1)\\ \mathbf{\Lambda}(s+1) & \mathbf{\Lambda}(s+2) & \cdots & \mathbf{\Lambda}(s+p+1) & \cdots & \mathbf{\Lambda}(s+q)\\ \vdots & \vdots & \ddots & \vdots & \cdots & \vdots\\ \mathbf{\Lambda}(s+p-1) & \mathbf{\Lambda}(s+p) & \cdots & \mathbf{\Lambda}(s+2p-1) & \cdots & \mathbf{\Lambda}(s+q+p-2)\end{bmatrix}\\ &= \begin{bmatrix}\mathbf{\Lambda}(s+p) & \mathbf{\Lambda}(s+p+1) & \cdots & \mathbf{\Lambda}(s+p+q-1)\end{bmatrix}\end{aligned} \quad \text{(B-6)}$$

The matrix representation of the above equation is

$$\mathbf{GT}_{1} = \mathbf{T}_{2} \quad \text{(B-7)}$$

where $\mathbf{G} \in \mathbf{R}^{m\times(m\times p)}$ is ARMA model parameter and can be rewritten as

$$\mathbf{G} = \left[-\mathbf{G}_1 \quad -\mathbf{G}_2 \quad \cdots \quad -\mathbf{G}_p \right] \tag{B-8}$$

where, $\mathbf{T}_1 \in \mathbf{R}^{(m\times p)\times(m\times q)}$, $\mathbf{T}_2 \in \mathbf{R}^{m\times(m\times q)}$, thus $\mathbf{G}$ is obtained by right multiplying $\mathbf{T}_1^T$ or $(\mathbf{T}_1\mathbf{T}_1^T)^{-1}$ on Eq.(B-7) we will obtain:

$$\mathbf{G} = \mathbf{T}_2 (\mathbf{T}_1 \mathbf{T}_1^{\ T})^{-1} \tag{B-9}$$

moreover, the coefficient matrix can be found by applying the singular value decomposition.

References

1) Nagamatsu, A.: *Mode Analysis*, Baihukan, 1985.
2) Okabayashi,T., Yamamori, K., Tamaru, Y., Yoshimura, T.: Estimation of dynamic characteristics for structures by the mobile vibration measurement system, *Journal of structural mechanics and earthquake engineering*, No.591/I-43, pp.327-337, 1998.
3) Okumatsu, T., Okabayashi, T., Fusamae, S., Funabara, Y., and Oiwane, K.: High accurate estimation of structural dynamic characteristics by the two-step structural identification method, *Journal of Structural Engineering* Vol.52A, pp.227-236, 2006.
4) Maruyama, O., Aisawa, S., Hoshiya, M.: Identification of dynamic properties of existing structures by mutivariate ARMA representation., *Journal of structural mechanics and earthquake engineering*, No.416/I-13, pp. 439-448, 1990.
5) Huang, C. S.: Structural identification from ambient vibration measurement using the multivariate AR model, *Journal of Sound and Vibration* Vol.241,No.3, pp. 337-359, 2001.
6) Hung, C. F., Ko, W. J., Peng, Y. T.: Identification of modal parameters from measured input and output data using a vector backward auto-regressive with exogeneous model, *Journal of Sound and Vibration* Vol.276, pp.1043-1063, 2004.
7) Ho, B. L. and Kalman, R. E.: Effective construction of linear state-variable models from input/output functions, *Regelungstechnik*, Vol.14, No.12, pp.545-548, 1966.
8) Faurre, P. L.: Stochastic realization algorithms, In system Identification: Advances and Case Studies, (R. Mehra and D. Lainiotis, eds) , Academic, pp.1-25, 1976.
9) Katayama, T.: *System Identification*, Asakura Shoten, 2004.
10) Juang, J. N. and Pappa, R. S.: An Eigensystem Realization Algorithm for Modal Parameter Identification and Model Reduction, *Journal of Guidance, Controlr, and Dynamics*, Vol. 9, No. 3, pp.294-303, 1986.
11) Juang, J. N.: *Applied System Identification*, Prentice Hall PTR, 1994.
12) Okabayashi,T., Naka, T., Okumatsu T., and Jiexin, H.: Estimation of structural dynamic properties by a multivariate autoregressive process with ambient vibration data, *Journal of structural mechanics and earthquake engineering* (under processing).
13) Ibrahim, S. R. and Mikulcik, E. C.: A method for the Direct identification of vibration parameters from the free response, *Shock and Vibration Bulletin* Vol.47, Part 4, pp.183-198, 1977.
14) Yang, Q. J., Zhang, P. Q., Li, C. Q. and Wu, X. P.: A system theory approach to multi-input multi-output modal parameters identification methods, *Mechanical System and Signal Processing*, Vol.8, No.2, pp.159-174, 1994.
15) Furukawa, T., Okabayashi, T., Kimura, K., and Okumatsu,T.: Estimation of traffic vibration level for existing bridge by using ARMA model, *Journal of structural mechanics and earthquake engineering*, No.787/I-71, pp.91-103, 2005.

(Received September 18, 2007)